Prospects for the Search for a Doubly-Charged Higgs in the Left-Right Symmetric Model with ATLAS

G. Azuelos[1,2], K. Benslama[3] and J. Ferland[1]

[1] Université de Montréal
[2] TRIUMF, Vancouver
[3] Nevis Labs, Columbia University

March 10, 2005

We estimate the potential for observation at the LHC of a doubly charged Higgs boson, as predicted in Left-Right symmetric models. Single production by vector boson fusion, $W^+W^+ \to \Delta^{++}_{L,R}$ and pair production by the Drell-Yan process $q\bar{q} \to \Delta^{++}_{L,R}\Delta^{--}_{L,R}$ are considered. Various decay channels are investigated: dileptons, including pairs of τ's, as well as WW.

1 Introduction

One major puzzle of the Standard Model is the fact that weak interaction couplings are strictly left-handed. In order to remedy this apparent arbitrariness of nature, one must extend the gauge group of the Standard Model to include a right-handed sector. The simplest realization is a Left-Right Symmetric Model (LRSM) [1] based on the group $SU(2)_L \otimes SU(2)_R \otimes U(1)_{B-L}$. Variants of this model derive generally from Grand Unified Theories [2], including superstring inspired models, based on extended groups which contain the LRSM as a subgroup. The breaking of $SU(2)_R \otimes U(1)_{B-L} \to U(1)_Y$ occurs at a high energy scale due to a triplet of complex Higgs fields [1] , consisting of Δ_R^0, Δ_R^+ and Δ_R^{++}, when its neutral component acquires a non-vanishing vacuum expectation value. The Higgs sector of the model therefore contains a doubly charged Higgs boson, which could provide a clean signature at the LHC since charge conservation prevents it from decaying to a pair of quarks. This will be the subject of the present work. For this purpose, we refer to previous phenomenological studies [4, 5, 6, 7], expanding the analyses by including the effects of backgrounds as well as detector acceptance and resolution. It must be noted that very light, $\mathcal{O}(\sim 100)$ GeV, doubly-charged Higgs particles can be expected in supersymmetric left-right models [8].

The LRSM has a number of interesting features. The enlarged symmetry group implies the existence of new heavy right-handed gauge bosons W_R and Z_R, while the fermion sector is enriched by representing the right-handed fermions as doublets in $SU(2)_R$. Yukawa couplings of the triplet Higgs allow for Majorana mass terms of the right-handed neutrinos, giving rise to the see-saw mechanism [9] as a natural explanation for the low, but non-vanishing mass of left-handed neutrinos. These heavy neutrinos further provide a mechanism for leptogenesis.

Other signatures of the LRSM have been studied in ATLAS. New heavy Z' gauge bosons can be observed in channels $Z' \to \ell^+\ell^-$ up to masses of 4.5 TeV [10, 11] with an integrated luminosity of 100 fb^{-1}. In analyses specific to the LRSM, the search of $W_R \to \ell\nu_R$ yields limits on the observability of the W_R and right-handed Majorana neutrino [12], as a function of the masses of these particles. The channel $Z_R \to \nu_R\nu_R \to \ell q\bar{q}'\ \ell q''\bar{q}'''$ should be observable [13] up to masses $M_{W_R} \lesssim$ 4 TeV and $m_{\nu_R} \lesssim 1.2$ TeV with 300 fb^{-1}. The new gauge bosons can also be searched for [14, 15] in the channels $Z_R \to WW \to e\nu jj$ and $W_R \to WZ$ if non-negligible mixing exists with the Standard Model (SM) gauge bosons. As a complement to these searches, observation of a doubly charged Higgs would clearly provide an important confirmation of the nature of the new physics.

The Higgs sector [4] of the LRSM consists of (i) the right-handed complex triplet Δ_R mentioned above, with weights (0,1,2), meaning singlet in $SU(2)_L$, triplet in $SU(2)_R$ and $B - L = 2$, (ii) a left-handed triplet Δ_L (1,0,2) (if the Lagrangian is to be symmetric under $L \leftrightarrow R$ transformation); and a bidoublet ϕ (1/2,1/2,0). The vacuum expectation values (vev) of the neutral members of the scalar triplets, v_L and v_R, break the symmetry $SU(2)_L \times SU(2)_R \to U(1)_Y$ as well as the discrete $L \leftrightarrow R$ symmetry. The non-vanishing vev of the bidoublet breaks the SM $SU(2)_L \times U(1)_Y$ symmetry. It is characterized by

[1] Alternative minimal Left-Right symmetric models exist with only doublets of scalar fields [3]. They do not lead to Majorana couplings of the right-handed neutrinos.

two parameters κ_1 and κ_2, with $\kappa = \sqrt{\kappa_1^2 + \kappa_2^2} = 246$ GeV. To prevent flavour changing neutral currents (FCNC), one must have $\kappa_2 \ll \kappa_1$, implying minimal mixing between W_L and W_R. The mass eigenstate of the singly charged Higgs is a mixed state of the charged components of the bidoublet and of the triplet.

In the analysis below, in order to have a manageable number of parameters, we relate the mass of W_R to v_R by: $m^2_{W_R} = g^2_R v^2_R/2$, which is a valid approximation in the limit where $v_L = 0$ and $\kappa_1 \ll v_R$. All the above parameters have bounds [7]: custodial symmetry constrains $v_L \lesssim 9$ GeV and present Tevatron lower bounds on M_{W_R} impose a limit $v_R > 1.4$ TeV, or $m_{W_R} > 650$ GeV, assuming equal gauge couplings $g_L = g_R$. Direct limits from the Tevatron on the mass of the doubly charged Higgs from di-leptonic decays have recently been reported in [16]. Indirect limits on the mass and couplings of the triplet Higgs bosons, obtained from various processes, are given in [17].

The paper is organized as follows: The next section discusses the phenomenology of the doubly charged Higgs at the LHC. Sect. 3 describes the methods of simulation of signals and background, as well as detector effects. The following two sections give results on the observability of the Δ_R^{++} and Δ_L^{++} respectively in various decay channels. The last section summarizes and concludes.

2 Phenomenology of the doubly-charged Higgs boson

Single production of a doubly charged Higgs at the LHC is possible via vector boson fusion, or via the fusion of a singly-charged Higgs with either a W or another singly charged Higgs, as shown in Fig. 1. The amplitudes of the W_LW_L and W_RW_R vector boson fusion processes are proportional to $v_{L,R}$. The other diagrams are suppressed by the Yukawa coupling of the Higgs to the quarks and by a coupling $\phi\phi\Delta$ proportional to the small parameter v_L. For the case of Δ_R^{++} production, the vector fusion process therefore dominates. For the production $WW \to \Delta_L^{++}$, the suppression due to the small value of the v_L is somewhat compensated by the fact that the incoming quarks radiate a lower mass vector gauge boson.

Double production of the doubly charged Higgs is also possible via a Drell-Yan process, with γ, Z or Z_R exchanged in the s-channel, but at a high kinematic price since enough energy is required to produce two heavy particles. In the case of Δ_L^{++}, double production may nevertheless be the only possibility if v_L is very small or vanishing.

The decay of a doubly charged Higgs can proceed by several channels. Dilepton decay provides a clean signature, kinematically enhanced, but the branching ratios depend on the unknown Yukawa couplings. Present bounds [7, 17] on the diagonal couplings $h_{ee,\mu\mu,\tau\tau}$ to charged leptons are consistent with values $O(1)$ if the mass scale of the triplet is large. For the Δ_L^{++}, this may be the dominant decay mode if v_L is very small. One would then have a golden signature: $q\bar{q} \to \gamma^*/Z^*/Z'^* \to \Delta_L^{++}\Delta_L^{--} \to 4\ell$. For very low Yukawa couplings ($h_{\ell\ell} \lesssim 10^{-8}$), the doubly charged Higgs boson could be quasi-stable, leaving a characteristic dE/dx signature in the detector, but this case is not considered here. The decay $\Delta_{R,L}^{++} \to W_{R,L}^+ W_{R,L}^+$ can also be significant. However, it is kinematically suppressed in the case of Δ_R^{++}, and suppressed by the small coupling v_L in the case of Δ_L^{++}. Furthermore, reconstruction of $W_{L,R}$ pairs is difficult at the LHC since they don't

produce a resonance and since W_R decays involving heavy Majorana neutrinos lead to complex events.

In the present work, we consider the production and decay modes discussed above. The results will be presented as limits in terms of the couplings v_L or v_R, taking fixed reference values for the Yukawa couplings of the doubly charged Higgs bosons to the leptons. It will then be a simple matter to re-interpret the results for different values of these Yukawa couplings. We will assume a truly symmetric Left-Right model, with equal gauge couplings $g_L = g_R = 0.64$. Since the mass of the W_R is essentially proportional to v_R, as mentioned in the introduction, it will not be an independent parameter.

We note that the existence of the Higgs triplet can also be detected in the decay channel $\Delta^+ \to WZ$. This will not be studied here, as the signal is very similar to narrow techicolor resonances which have been analyzed elsewhere [18].

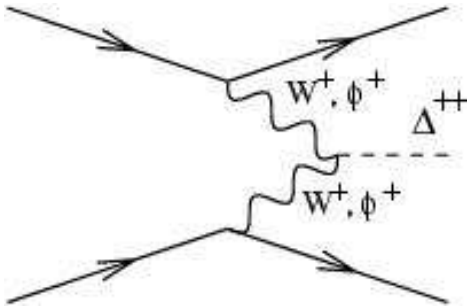

Figure 1: Feynman diagrams for single production of Δ^{++}

3 Simulation of the signal and backgrounds

The processes of single and double production of doubly charged Higgs are implemented in the PYTHIA generator [19]. Events were generated using the CTEQ5L parton distribution functions, taking account of initial and final state interactions as well as hadronization. The following processes were studied here:

- $W^+_{R,L}W^+_{R,L} \to \Delta^{++}_{R,L} \to e^+e^+/\mu^+\mu^+$
- $W^+_{R,L}W^+_{R,L} \to \Delta^{++}_{R,L} \to \tau^+\tau^+$ with one or both τ's decaying leptonically.
- $q\bar{q} \to \gamma^*/Z_{R,L} \to \Delta^{++}_{R,L}\Delta^{--}_{R,L}$

The process $W^+_{R,L}W^+_{R,L} \to \Delta^{++}_{R,L} \to W^+_{R,L}W^+_{R,L}$ has not been considered. The case of left-handed W's was previously studied [20] in the framework of the little Higgs model and is discussed briefly in Sect. 5.2.

Detector effects and acceptance were simulated using ATLFAST [22], a fast simulation program for the ATLAS detector. Conditions of high luminosity ($\mathcal{L} = 10^{34}$ cm^{-2} s^{-1}) were assumed. Jets were reconstructed from calorimeter clusters using a cone algorithm, with

a cone radius $\Delta R = \sqrt{(\Delta\eta)^2 + (\Delta\phi)^2} = 0.4$. Charged leptons (electrons and muons) were reconstructed within the acceptance range in pseudorapidity $|\eta| < 2.5$. They were considered isolated if they were separated by $\Delta R > 0.4$ from other clusters and if, within a cone of radius 0.2, less than 10 GeV transverse energy was deposited. An efficiency of reconstruction of 90% was assumed for these leptons. Reconstruction of τ jets assumed an efficiency of 40% with a corresponding mistagging probability of ∼0.05% for a central τ jet having 100 GeV of transverse momentum. For b-jets, the tagging efficiency was taken as 50%, with a mistagging probability of light quark jets of 1/230.

The principal backgrounds depend on the production and decay process under consideration. PYTHIA was used to generate $t\bar{t}$ production, which has a very large cross section of 500 pb. Other backgrounds were simulated using the CompHep generator [21]: (i) The process $qq \to W^+W^+qq$ was produced with cuts at generation requiring transverse momentum of the outgoing quarks to be > 15 GeV and an invariant mass of the W^+W^+ system greater than 200 GeV. CTEQ5L parton density functions were used, with $Q^2 = m_W^2$. With an assumed Higgs mass of 120 GeV, the contribution of longitudinal gauge boson scattering is very small. (ii) $qq \to W^+Zqq$ was generated under similar conditions. (iii) Finally the process $pp \to Wt\bar{t}$ was also generated with CompHep. The cross sections of these processes are given in Table 2.

A number of systematic uncertainties, some of which are difficult to evaluate reliably before experimental data are available, will apply. No k-factors have been used here, although next-to-leading-order corrections can be substantial for these high mass resonance states. The luminosity measurement is expected to have a precision of $\sim 5 - 10\%$. The efficiency of lepton reconstruction in ATLAS, here taken to be 90%, will have to be better understood. The energy resolution, especially for high energy electrons, must be evaluated with full detector simulation and optimized reconstruction algorithms. Charge misidentification was not included here since it is small ($\sim 5\%$ for leptons having a transverse momentum of 1 TeV).

4 Search for Δ_R^{++}

A different analysis strategy has been applied for each of the four modes of production and decay of the bileptons described in Sect. 2. As mentioned above, since the Yukawa couplings to leptons are not known, we will not account for branching ratios into the various decay channels, but the reach on the parameter v_R could be recomputed trivially for any given values of these branching ratios.

We will only consider signals for doubly positively charged Higgs bosons, as they are about 1.6 times more abundant than the negatively charged ones, at the LHC (see Table 1). The same ratio of positively charged to negatively charged leptons can be expected from the backgrounds, to the extent that $qqWW$ dominates, and hence the improvement in the significances obtained below can be estimated at 22%.

M(Δ_R^{++})	% of ++
300	64.5
500	67.5
800	71.5
1000	75.3
1500	79.1

Table 1: Percentage of positively charged Δ_R as a function of mass. A value $m_{W_R} = 650$ GeV was assumed.

4.1 Dilepton channel

The backgrounds relevant to the two-lepton channel are shown in Table 2. A requirement of the presence of at least two leptons (e or μ) has been applied, except for the $t\bar{t}$ sample, where only one lepton was required. Although the cross sections are quite large, compared to those of the signal, given in Table 3, they can be effectively suppressed by appropriate cuts, as will be seen below.

Background	Number of Events	$\sigma \times BR$ (fb)
pp $\rightarrow$ W$t\bar{t}$	200 000	23
qq $\rightarrow W^+W^+\ qq$	100 000	37
qq $\rightarrow$ WZqq	27 000	28.6
qq $\rightarrow t\bar{t}$ $\quad P_t$ 10-200 GeV	8 000 000	90 800
qq $\rightarrow t\bar{t}$ $\quad P_t$ 200 GeV-∞	2 000 000	14 100

Table 2: Background processes for the dilepton channel. The third column gives $\sigma \times BR$, where BR is the branching ratio to a final state with at least two leptons, except for $t\bar{t}$ where only one lepton is required. The number of events used for the analysis is also shown.

4.1.1 $\Delta_R^{++} \rightarrow e^+e^+/\mu^+\mu^+$

The selection criteria for this channel were the following:

1. Two isolated leptons ($\ell = e, \mu$) of positive charge were required. The ATLAS trigger requires that at least one of the leptons must have a transverse momentum > 25 GeV. The invariant mass of the two leptons, $M_{\ell\ell}$, was then computed.

2. Since the leptons are expected to be energetic, an additional requirement that both of them have a transverse momentum $p_T > 50$ GeV was imposed.

3. The total transverse energy of the two leptons is correlated with the mass of the Δ_R^{++} from which they originate (see Fig. 2). A mass-dependent cut was therefore applied: $\alpha(p_T^{\ell_1} + p_T^{\ell_2}) - M_{\ell\ell} = \beta$, where the values $\alpha = 2.4$ and $\beta = 480$ GeV were chosen to suppress background without significant loss of signal

M(W_R^+)	M(Δ_R^{++})				
	300	500	800	1000	1500
650	7.9	4.6	2.2	1.4	0.45
750	4.7	2.8	1.4	0.87	0.31
850	2.9	1.8	0.90	0.58	0.21
950	1.9	1.2	0.61	0.40	0.15
1000	1.6	0.98	0.50	0.33	0.12
1050	1.3	0.81	0.42	0.28	0.11
1500	0.30	0.20	0.11	0.074	0.029

Table 3: Cross section (fb) for the process $p + p \to \Delta_R^{\pm\pm}$ as a function of the mass of the Δ and of the W_R.

4. The two partons from which the vector bosons have been radiated are expected to produce jets of high energy in the forward and backward regions. A forward jet tag was therefore required:

   (a) After ordering all the jets with $p_T > 15$ GeV in decreasing order of energy, the first one, j_1, was considered a candidate forward-tagged jet if its energy was higher than 200 GeV.

   (b) Looping over the remaining jets, the second candidate forward-tagged jet, j_2, was identified if its angular separation from j_1 satisfied $|\eta_{j_1} - \eta_{j_2}| > 2$ and if its energy was greater than 100 GeV.

   The above requirements for "forward jets" are loose, but were found to be sufficient for the present purpose.

5. The missing transverse energy was required to be less than 100 GeV. This cut was not applied for cases $\Delta_R^{++} > 800$ GeV since it was not needed to reduce the background.

Table 4 shows the number of events expected from the various backgrounds and for typical cases of signal where $m_{\Delta_R^{++}} = 300$ or 800 GeV and $m_{W_R^+} = 650$ GeV, after successive application of the cuts. A window of $\pm 2\times$ the width of the reconstructed mass of the Δ_R^{++} was selected. The numbers are normalized to a luminosity of 100 fb^{-1}. Fig. 3 shows the distribution of $m_{\Delta_R^{++}}$ and backgrounds for the case $m_{\Delta_R^{++}} = 800$ GeV.

Since the background is negligible, discovery can be claimed if the number of signal events is 10 or higher. With this definition, the contour of discovery, in the plane $m_{W_R^+}$ versus $m_{\Delta_R^{++}}$ (or v_R) has been estimated from a sample of test cases. The discovery reach at the LHC is shown in Fig. 4, for integrated luminosities of 100 fb^{-1} and 300 fb^{-1} and assuming 100% BR to lepton pairs.

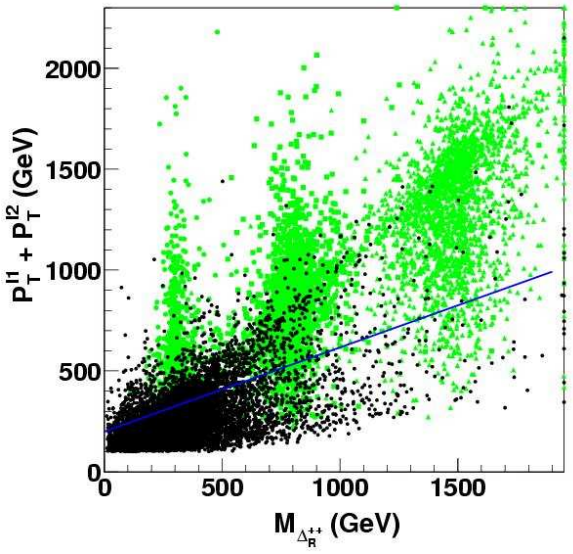

Figure 2: Distribution of the scalar sum of the two lepton transverse energies as a function of their invariant mass. In green (light shade) are shown the distributions for signals of $m_{\Delta_R^{++}} = 300, 800$ and 1500 GeV and m_{W_R}=650 GeV. The sum of the backgrounds is in black. The straight line indicates where the mass-dependent cut is applied.

4.1.2 $\Delta_R^{++} \to \tau^+\tau^+$

It is possible that the predominant decay of the Δ_R^{++} will be to the third generation leptons if the Yukawa couplings are proportional to mass. For this important decay channel, the cleanest signal of $\Delta_R^{++} \to \tau^+\tau^+$ will be the one where the two $\tau's$ decay leptonically. Although neutrinos are involved in the process, the mass of the tau pair can be reconstructed, as was done for example in $H/A \to \tau\tau$ studies [11]. One must neglect the mass of the τ lepton and assume that the neutrinos from the decay $\tau \to \ell\nu_\ell\nu_\tau$ are collinear with the charged lepton. This is a good approximation to the extent that Δ_R^{++} is heavy and the $\tau's$ are highly boosted. Defining $x_{\tau 1}$ and $x_{\tau 2}$ as the respective fractions of tau energy carried by the charged lepton, conservation of transverse momentum yields values for these variables and the invariant $\tau\tau$ mass can then be calculated:

$$m_{\tau\tau} = \frac{m_{\ell\ell}}{\sqrt{x_{\tau 1} x_{\tau 2}}} \tag{1}$$

Since the energies involved here are large, it is not expected that this method of $\tau\tau$ mass reconstruction will depend much on the precision with which missing transverse energy can be measured, taken here from fast simulation.

The same method of reconstruction applies for 1-prong or 3-prong hadronic decays of the τ.

$\underline{\tau^+\tau^+ \to \ell^+\ell^+ p_T^{miss}}$

	Δ^{++} 300 GeV	Δ^{++} 800 GeV	$W^+W^+\,qq$	$W\,t\bar{t}$	$WZqq$	$t\bar{t}$	total backg
Isolated leptons	278 (327)	63 (95)	109/12	7.6/0.6	0/0.8	17/0	133/13
Lepton P_T	256 (301)	63 (94)	63/11	5.9/0.5	0/0.8	1.1/0	70/12
$2.4(P_T^{l_1}+P_T^{l_2})-M_{ll}>480$	191(227)	59(85)	10/2.1	1.3/0.3	0	0	12/2.4
Fwd Jet tagging	156(186)	56(74)	6.0/1.3	0.1/0	0	0	6/1.3
ptmiss	154(181)	56(68)	3.0/0.3	0/0	0	0	3.1/0.3

Table 4: Number of events of signal and backgrounds after successive application of cuts, for the case $\Delta_R^{++}\to\ell^+\,\ell^+$, for $m_{\Delta_R^{++}}=300$ GeV and 800 GeV and $m_{W_R}=650$ GeV and for 100 fb^{-1}. Mass windows $\pm 2\sigma$ around the resonances have been chosen. In parentheses is shown the number of events without the mass window cut.

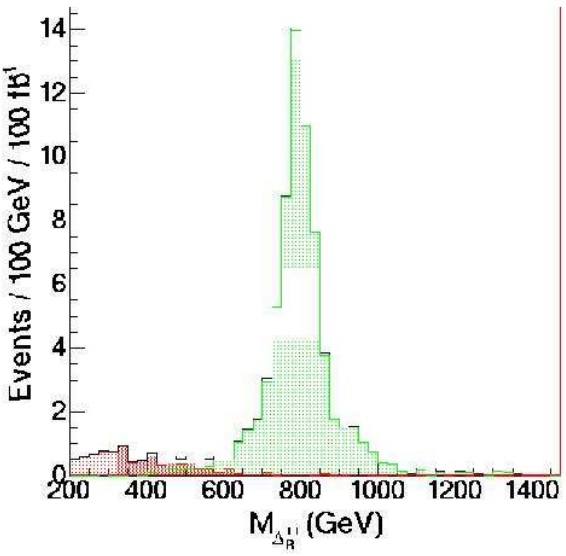

Figure 3: Reconstructed invariant mass of the two leptons from the process $W^+W^+\to\Delta_R^{++}\to\ell^+\ell^+$. The signal (green) is for a mass $m_{\Delta_R^{++}}=800$ GeV with $m_{W_R}=650$ GeV and the background is in red. The black histogram is the sum of both. The distributions are for 100 fb^{-1}.

Assuming 100% decay of Δ_R^{++} to tau pairs, the cross section for the process $p+p\to\Delta_R^{\pm\pm}\to\tau\tau\to\ell\nu\nu\;\ell\nu\nu$ is the same as in Table 3, but the branching ratio BR($\tau\to\ell\nu\nu$) of 35% per τ must be taken into account. Besides the backgrounds of Table 2, we have also taken into account Zjj, for which details on the generation can be found in [23].

The following selection criteria were applied to extract the signal from the backgounds:

1. two isolated leptons of the same charge were required in the event, with $p_T>25$ GeV. The event trigger is thus satisfied.

2. the calculated variables $x_{\tau 1}$ and $x_{\tau 2}$ were required to lie within the physical range

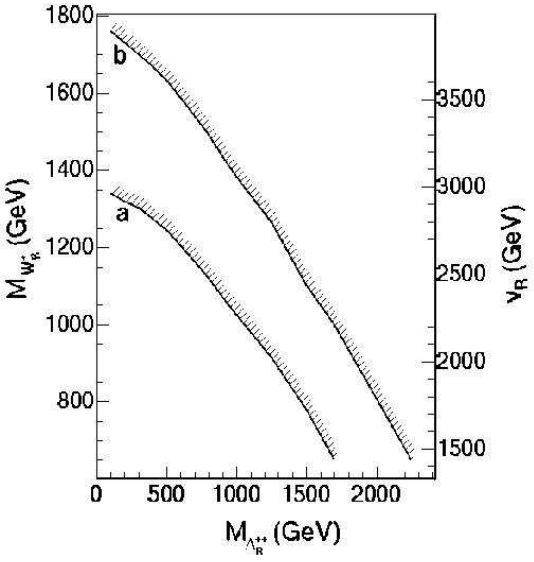

Figure 4: Discovery reach for $\Delta_R^{++} \to l^+l^+$ in the plane $m_{W_R^+}$ versus $m_{\Delta_R^{++}}$ (or v_R) for integrated luminosities of 100 fb^{-1}(a) and 300 fb^{-1}(b), and assuming 100% BR to dileptons.

$0 \leq x_{\tau i} \leq 1$. Events for which sources of missing energy other than the neutrinos from the two tau decays are present, or for which the collinear approximation made above is not valid, will be lost.

3. in order to reduce the $t\bar{t}$ background, the event was rejected if a b-tagged jet was present.

4. forward jet tagging was required as in Sect. 4.1.1

5. Missing transverse momentum was required to be at least 150 GeV

Table 5 shows the number of events expected from the various backgrounds and for the cases of signals where $m_{\Delta_R^{++}} = 300$ and 800 GeV and $m_{W_R^+} = 650$ GeV, after successive application of the cuts. A window of $\pm 2\times$ the width of the reconstructed mass of the Δ_R^{++} was selected. Fig. 5 shows the distribution of $m_{\Delta_R^{++}}$ and backgrounds for $m_{\Delta_R^{++}} = 800$ GeV. A significance $S/\sqrt{B}$ of only about 4.3 is obtained in this case for an integrated luminosity of 100 fb^{-1}. With simultaneous search for the Δ_R^{--}, and with 300 fb^{-1}, the significance should reach 9.1. Contours of discovery in this channel, defined as a 5σ significance with at least 10 events, is shown in Fig. 6. We note that they are weaker than for $\Delta_R^{++} \to \ell^+\ell^+$ of Fig. 4, and do not cover a large region of mass which is unconstrained ($m_{W_R} > 650$ GeV). However, it may help to confirm discovery, or may be more applicable if the coupling to τ's dominates.

	Δ^{++} 300 GeV	Δ^{++} 800 GeV	$W^+W^+\,qq$	$W\,t\bar{t}$	$WZqq$	$t\bar{t}$	total backg
Isolated leptons	44 (49)	20 (23)	153/80	13/5.1	12/0.7	486/137	707/234
$0 < x_{\tau 1},\ x_{\tau 2} < 1$	44 (46)	20 (21)	84/60	6.4/3.3	8.0/0.7	360/101	480/171
no b-jet	42 (44)	18(21)	84/59	0.2/0.2	7.2/0.7	62/16	175/83
Fwd Jet tagging	36 (34)	16 (18)	21/15	0/0	2.3/0	20/7.4	45/23
$E_T^{miss} > 150$ GeV	23 (25)	13 (15)	5.2/7.2	0/0	0.8/0	2.5/2.1	8.6/9.3

Table 5: Number of events of signal and backgrounds after successive application of cuts, for the case $\Delta_R^{++} \to \tau^+\tau^+ \to \ell\nu\ \ell\nu$, for $m_{\Delta_R^{++}} = 300$ GeV and 800 GeV and $m_{W_R} = 650$ GeV, for 100 fb^{-1}. Mass windows $\pm 2\sigma$ around the resonances have been chosen. In parentheses is shown the number of events without the mass window cut.

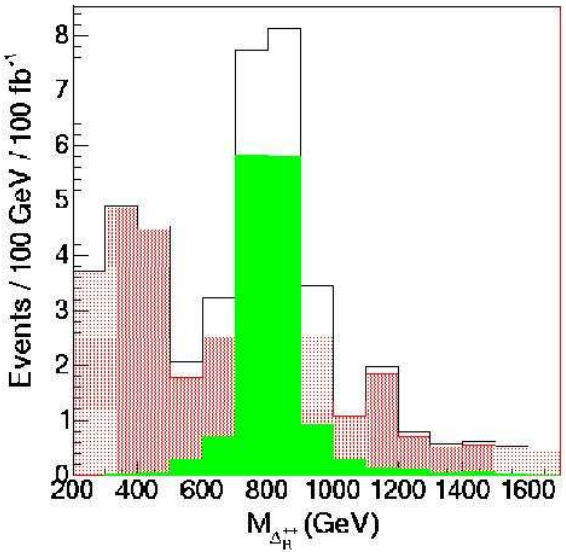

Figure 5: Reconstructed mass of the Δ_R^{++} from the decay channel $\Delta_R^{++} \to \tau^+\tau^+ \to \ell^+\ell^+ + P_T^{miss}$. In red (light shade) and green (dark shade) are shown the background and the signal, for an integrated luminosity of 100 fb^{-1}. The solid black histogram is the sum.

$\tau^+\tau^+ \to \ell^+ h p_T^{miss}$

Analysis of this channel shows that the background from W + jets will completely dominate the signal. Therefore, it will not be discussed here, but details can be found in [24].

4.2 Pair production $\Delta_R^{++}\Delta_R^{--} \to 4\ell$

Pair production of $\Delta_R^{++}\Delta_R^{--}$ is suppressed by the expected high mass of the Δ_R^{++} but can nevertheless serve to confirm discovery in some region of mass. The diagrams with s-channel Z and Z' exchange have been added to the γ exchange diagram in the implementation of the Drell-Yan process in the PYTHIA generator, taking the coupling of

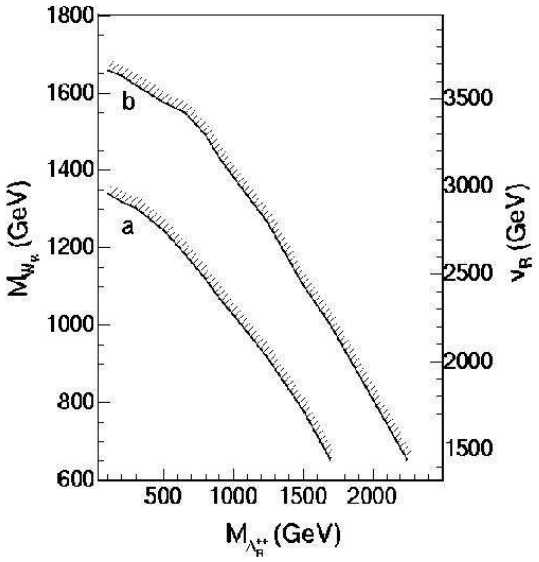

Figure 6: Discovery reach in the plane m_{W_R} vs $m_{\Delta_R^{++}}$ (or v_R) in the decay channel $\Delta_R^{++} \to \tau^+\tau^+ \to \ell^+\ell^+ + P_T^{miss}$ for integrated luminosities of 100 fb^{-1}(a) and 300 fb^{-1}(b).

Z, Z' to fermions and to Δ_L^{++} from references [25, 5]. In principle, the branching ratio depends on the assumed mass of Δ_L^{++}, as well as that of Δ_R^{++}, but since the Z' has a large partial width to fermions, such that $BR(Z' \to \Delta^{++}\Delta^{--})$ is of the order of 1%, the contribution of these decay channels to the total width of the Z' was neglected. For the case of leptonic decays of the doubly-charged Higgs bosons, the process constitutes a golden channel and the background will be negligible. Fig. 7 shows the contours of discovery, defined as observation of 10 events, if all four leptons are detected or if any 3 of the leptons are observed. Being an s-channel process not involving the W_R, this channel is not sensitive to the mass of this heavy gauge boson.

4.3 Other channels

Other possible channels have not been considered here. Single production followed by the decay $\Delta_R^{++} \to W_R^+ W_R^+$ is possible if $m_{\Delta_R^{++}}$ is sufficiently large, but given the lower bound on m_{W_R}, this channel is strongly suppressed kinematically. It would be also difficult to reconstruct since the decays $W_R \to \ell N$ would not lead to a mass resonance and would require a knowledge of the mass of N, a heavy right-handed or Majorana neutrino. Pair production $\Delta_R^{++}\Delta_R^-$ and other such combinations can arise from s-channel W exchange and can complete the study of Sect. 4.2

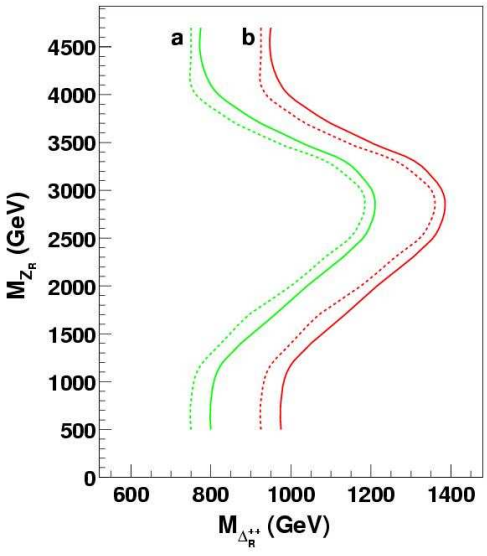

Figure 7: Contours of discovery for 100 fb^{-1}(a) and for 300 fb^{-1}(b) in the plane $m_{Z'}$ vs $m_{\Delta_R^{++}}$. The dashed curves are for the case where all four leptons are observed, and the full curves are when only three leptons are detected.

5 Search for Δ_L^{++}

5.1 Dilepton channel

As for the case of the Δ_R^{++} the dilepton channel provides a clean signature. Although the Yukawa coupling of Δ_L^{++} to leptons remains a parameter of the theory, this channel can, in fact, be dominant since the alternative decay to gauge bosons is possibly negligible, being proportional to the very small value of the vev v_L. In the limit where $v_L = 0$, it will be the only open channel, but production of Δ_L^{++} will only occur in pairs, through s-channel $\gamma/Z/Z'$ exchange. As before, we will assume below 100% branching ratio to leptons, but results can be reinterpreted in a straightforward way for different values of this branching ratio.

The production cross section of Δ_L^{++} is proportional to v_L^2. Table 6 gives the value as a function of mass, for $v_L = 9$ GeV.

M($\Delta_L^{\pm\pm}$)					
300	400	500	600	700	800
9.847	6.155	4.057	2.822	2.024	1.494

Table 6: Cross section (fb) for the process $p + p \to \Delta_L^{\pm\pm}$ as a function of the mass of the Δ for $v_L = 9$ GeV.

5.1.1 $\Delta_L^{++} \to e^+e^+/\mu^+\mu^+$

The following selection criteria were applied:

1. Two isolated leptons (e or μ) of positive sign must be reconstructed, with $p_T > 25$ GeV

2. Since the leptons result from the decay of a heavy, slow particle, they will be collinear. The azimuthal separation between the two leptons is required to satisfy the cut $\Delta\Phi_{ll} > 2.5$ when the reconstructed mass is 300 GeV or more. For lower masses, we choose $\Delta\Phi_{ll} > 1$ (see Fig. 8).

3. The vectorial difference between the transverse momenta of the two leptons ($\Delta_{P_T^{ll}}$)is tuned for each assumed mass of the reconstructed Δ_L^{++}. We require: $\Delta_{P_T^{ll}} > (\frac{M_{ll}}{2}+50)$ for masses 200 GeV or more and $\Delta_{P_T^{ll}} > 70$ GeV otherwise (see Fig. 9).

4. Forward jet tagging is applied as in Sect. 4.1.1.

5. The missing energy is required to be less than 40 GeV since, in the SM, a same-sign lepton pair will always be associated with missing energy from accompanying neutrinos. In addition, we reject events where one jet is tagged as a b-jet.

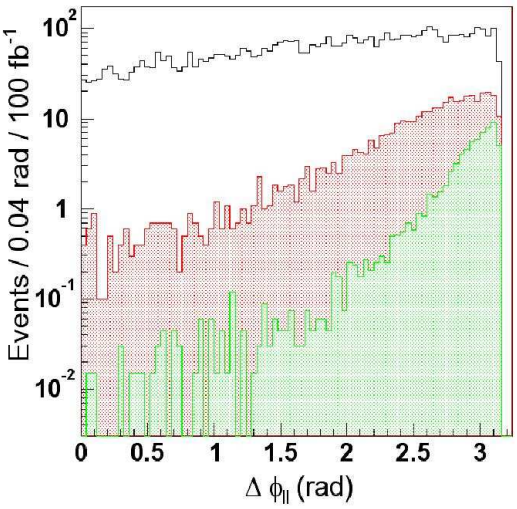

Figure 8: $\Delta\Phi_{ll}$ for a Δ_L^{++} of mass 300 GeV in red (dark shade) and for a mass of 800 GeV in green (light shade), as well as the standard model background.

Table 7 gives the number of expected signal and background events for the cases $m_{\Delta_L^{++}} = 300$ GeV and $m_{\Delta_L^{++}} = 800$ GeV respectively. A mass window of $\pm 2\times$ the width of the resonance was selected. An example of a signal over SM background is given in Fig. 10. The discovery reach in the plane v_L vs $m_{\Delta_L^{++}}$ is shown in Fig. 11.

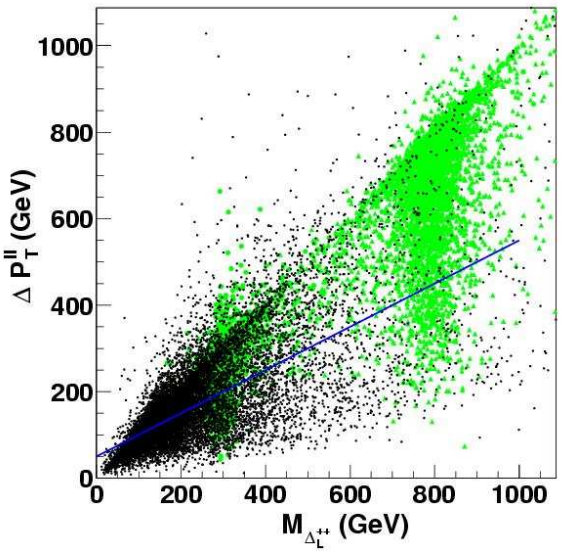

Figure 9: Distribution of the scalar sum of the two lepton transverse energies as a function of their invariant mass in the case $\Delta_L^{++} \to \ell\ell$. In green (light shade) are shown the distributions for signals of $m_{\Delta_L^{++}} = 300$ and 800 GeV. The sum of the backgrounds is in black. The straight line indicates where the mass-dependent cut is applied.

5.1.2 $\Delta_L^{++} \to \tau^+\tau^+$

As mentioned above, the Yukawa coupling of Δ_L^{++} to τ leptons may dominate, in which case it will be essential to reconstruct the decay $\Delta_L^{++} \to \tau^+\tau^+$. As for the case of Δ_L^{++} presented above, besides the backgrounds of Table 2, we have also taken into account Zjj.

$\underline{\tau^+\tau^+ \to \ell^+\ell^+ p_T^{miss}}$

The following cuts have been applied to select the di-lepton final states:

1. two same sign leptons with $P_T > 25$ GeV.
2. Tau reconstruction: $0 < x_{\tau 1} < 1$ and $0 < x_{\tau 2} < 1$, where $x_{\tau 1,\tau 2}$ are defined as in Sect. 4.1.2
3. b-jet veto: a b-jet tagging efficiency of 0.6 is applied
4. forward jet tagging, as in Sect. 4.1.1
5. in order to reduce the $t\bar{t}$ and $qqWW$ backgrounds an additional cut was applied on the invariant mass of the two leptons: $M_{l1l2} > 30$ GeV

Results of the analysis for a $\Delta_L^{++}$of mass of 300 GeV and 800 GeV are summarized in Table 8. A mass window of $\pm 2\times$ the width of the reconstructed resonance has been

	Δ^{++} 300 GeV	Δ^{++} 800 GeV	total backg
Isolated leptons	330 (384)	59 (69)	133/13
$\|\Delta\phi_{\ell\ell} > 2.5\|$	253 (289)	56 (65)	75/8.3
$\Delta_{P_T^{ll}} > (\frac{M_{ll}}{2}+50)$	220 (260)	50 (59)	37/2.5
Fwd Jet tagging	156(185)	40 (47)	17/1.4
ptmiss	152(180)	34 (40)	3.0/0.1

Table 7: Number of events of signal and total background after successive application of cuts, for the case $\Delta^{++} \to \ell^+ \ell^+$, for $m_{\Delta_L^{++}} = 300$ GeV and 800 GeV and $m_{W_R} = 650$ GeV, for 100 fb^{-1}. Mass windows $\pm 2\sigma$ around the resonances have been chosen. In parentheses is shown the number of events without the mass window cut.

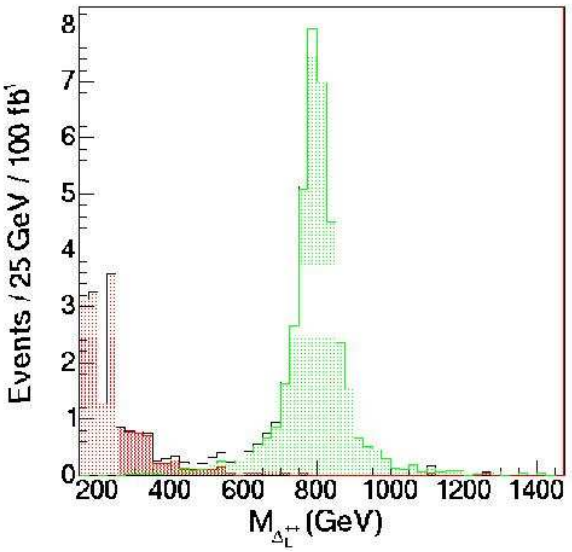

Figure 10: Reconstructed invariant mass of the two leptons from the process $W^+W^+ \to \Delta_L^{++} \to \ell^+\ell^+$. The signal (green) is for a mass $m_{\Delta_R^{++}} = 800$ GeV and the background is in red. The black histogram is the sum of both. The distributions are for 100 fb^{-1} and $v_L = 9$.

selected. The parameter region where discovery is possible with 100 fb^{-1} is shown in Fig. 12.

$\underline{\tau^+\tau^+ \to \ell^+ h p_T^{miss}}$

As for the case of Δ_R^{++} discussed above, this channel is dominated by W + jets background and will not been shown here. Details can be found in [24].

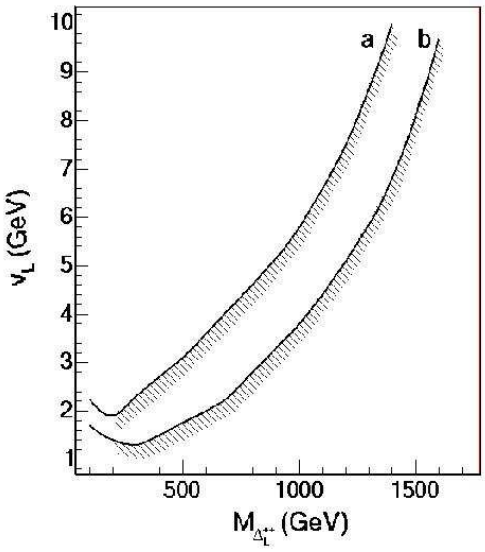

Figure 11: Discovery reach for $\Delta_L^{++} \to \ell^+\ell^+$ in the plane v_L versus $m_{\Delta_L^{++}}$ for integrated luminosities of 100 fb^{-1}(a) and 300 fb^{-1}(b) and assuming 100% BR to dileptons.

5.2 $\Delta_L^{++} \to W^+W^+$

The decay of Δ_L^{++} to a pair of W bosons has been previously analyzed in the context of the little Higgs model [20] and will not be repeated here. It was found that the background from the qqW^+W^+ production process (with transverse W's) was significant and that a 1 TeV resonance could be discovered at the LHC in this channel, with an integrated luminosity of 300 fb^{-1}, only if $v_L > 29$ GeV. This value of v_L is higher than would be reasonably expected from the constraints on the ρ parameter, as mentioned in the introduction.

5.3 Pair production $\Delta_L^{++}\Delta_L^{--}$

As for the case of the right-handed sector, pair production of Δ_L is a possible discovery channel. The diagram with s-channel Z' exchange has been added to the implementation of this Drell-Yan process in the PYTHIA generator, taking the coupling of Z' to fermions and to Δ_L^{++} from references [5, 25]. Assuming leptonic decays, the background will be negligible. Fig. 13 shows the contours of discovery, defined as observation of 10 events, if all four leptons are detected or if any 3 of the leptons are observed.

6 Summary and Conclusion

Left-Right symmetric models predict the existence of doubly-charged Higgs bosons which should yield a striking signature at the LHC. The principal possible production and decay

	Δ^{++} 300 GeV	Δ^{++} 800 GeV	total backg
Isolated leptons	42 (54)	10.1(13.4)	707/299
$0 < x_1,\ x_2 < 1$	40 (47)	9.6 (12.0)	480/222
no b jet	38 (46)	9.1 (11.5)	158/100
Fwd Jet tagging	18 (22)	4.3 (5.8)	33/23
$M_{ll} > 30$ GeV	15 (16.3)	3.8 (4.8)	23/16

Table 8: Number of events of signal and backgrounds after successive application of cuts, for the case $\Delta_L^{++} \to \tau^+\tau^+ \to \ell\nu\ \ell\nu$, for $m_{\Delta_L^{++}} = 300$ GeV and 800 GeV and $v_L = 9$, for 100 fb^{-1}. Mass windows $\pm 2\sigma$ around the resonances have been chosen. In parentheses is shown the number of events without the mass window cut.

modes have been investigated and the reach of ATLAS for discovery is summarized in Figs. 4, 6, 7, 11 and 12 in terms of the parameters of the model. These plots are not independent. As the couplings to fermions are not known, the different channels have been considered separately, assuming 100% branching ratio in each case.

It is found that the LHC will be able to probe a large region of unexplored parameter space in the triplet Higgs sector. This analysis complements previous ATLAS studies searching for signals of the Left-Right symmetric model.

7 Acknowledgments

This work has been performed within the ATLAS collaboration. We have made use of physics analysis and simulation tools which are the result of collaboration-wide efforts. We would like to thank Pierre-Hugues Beauchemin and Nathaniel Lubin for their help. K.B. acknowledges support from the National Science Foundation USA, and G.A. from NSERC Canada.

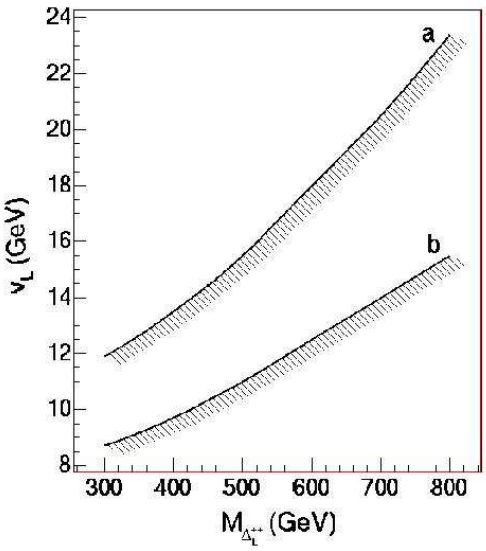

Figure 12: Discovery reach, in the plane v_L versus $m_{\Delta_L^{++}}$ for integrated luminosities of 100 fb^{-1}(a) and 300 fb^{-1}(b) and assuming 100% BR to dileptons.

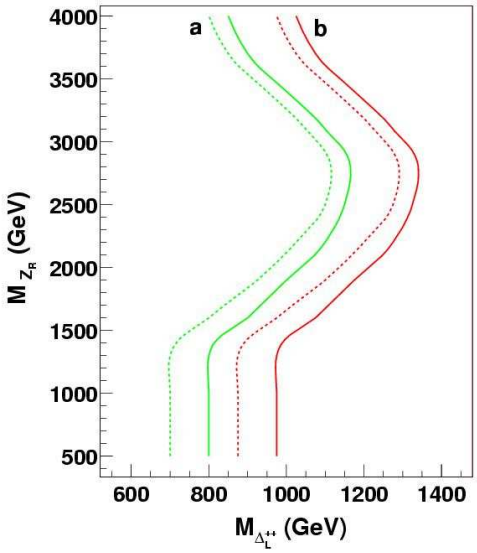

Figure 13: Contours of discovery in the plane $m_{Z'}$ vs $m_{\Delta_L^{++}}$ for 100 fb^{-1}(a) and 300 fb^{-1}(b). The dashed curves are for the case where all four leptons are observed, and the full curves are when only three leptons are detected.

References

[1] R.N. Mohapatra and J. C. Pati, Phys. Rev. **D11** (1975) 566

[2] J. Pati and A. Salam, Phys. Rev. **D8**, (1973) 1240; see also references in the PDG review by S. Raby in Phys. Rev. D66 (2002) 010001-142 and in R. N. Mohapatra, *Unification and Supersymmetry, The Frontiers of Quark-Lepton Physics*, Third edition, Springer 2003.

[3] K.S. Babu and R.N. Mohapatra, Phys. Rev. **D41** (1990) 1286 and references therein; Y.A. Couthinho, J.A. Martins Simões and C. M. Porto, Eur. Phys. J. **C18** (2001) 779 B. Brahmachari, E. Ma and U. Sarkar, Phys. Rev. Lett. **91** (2003) 011801.

[4] J.F. Gunion *et al.* Phys. Rev. **D40** (1989) 1546.

[5] J.A. Grifols, A. Méndez and G.A. Schuler, Mod. Phys. Lett. **A4** (1989) 1485.

[6] R. Vega and D.A. Dicus, Nucl Phys. **B329** (1990) 533.

[7] K.Huitu, J.Maalampi, A.Pietilä and M.Raidal, Nucl.Phys. **B487** (1997) 27-42 (hep-ph/9606311).

[8] C.S. Aulakh, A. Melfo and G. Senjanovic, Phys. Rev. **D57** (1998) 4174; Z. Chacko and R. Mohapatra, Phys. Rev. **D58** (1998) 015003.

[9] R.N. Mohapatra and G. Senjanović, Phys. Rev. **D23** (1981) 165.

[10] The limit in fact depends on the existence of exotic decay modes. The approximate value given here is an extrapolation, using appropriate Z' couplings, from: M.C. Cousinou, ATL-PHYS-94-059; A. Henriques and L. Poggioli, ATL-PHYS-92-010.

[11] ATLAS Detector and Physics Performance Technical Design Report, CERN/LHCC/99-15, May 1999.

[12] J. Collot and A. Ferrari, ATL-PHYS-99-018 (also PhD Thesis of A. Ferrari).

[13] A. Ferrari and J. Collot, ATL-PHYS-2000-034.

[14] D. Benchekroun, C. Driouichi and A. Hoummada, SN-ATLAS-2001-001 published in EPJdirect **C3**, 1 (2001) DOI 10.1007/s1010501c0003.

[15] E. Arik *et al.*, ATL-PHYS-2001-005.

[16] D0 Collaboration, V.M. Abazov *et al.*, Phys. Rev. Lett. **93** (2004) 141801; CDF Collaboration, D. Acosta *et al.*, Phys. Rev. Lett. **93** (2004) 221802.

[17] M.L. Swartz, Phys. Rev. **D40** (1989) 1521.

[18] G. Azuelos, P. Depommier, R. Mazini and K. Strahl, ATL-PHYS-99-020.

[19] T. Sjöstrand, P. Edén, C. Friberg, L. Lönnblad, G. Miu, S. Mrenna and E. Norrbin, Computer Physics Commun. 135 (2001) 238.

[20] G. Azuelos et*al.*, SN-ATLAS-2004-038, European Phys Journal C (2004) 10.1140/epjcd/s2004-02-002-x (hep-ph/0402037); G. Azuelos, K. Benslama and G. Couture, ATL-PHYS-2004-002.

[21] *CompHEP - a package for evaluation of Feynman diagrams and integration over multi-particle phase space*, A.Pukhov, *et al.*, INP MSU 98-41/542, (hep,ph/9908288).

[22] *ATLFAST, a fast simulation package for ATLAS*, E. Richter-Was, D. Froidevaux and L. Poggioli, ATLAS internal note ATL-PHYS-98-131.

[23] R. Mazini and G. Azuelos, *Searching for* $H \to \tau\tau l\nu\nu_\tau + hX$ *by vector boson fusion in ATLAS* ATL-PHYS-2003-004.

[24] J. Ferland, M.Sc. Thesis, Université de Montréal, to be submitted.

[25] F. Cuypers, Spring School on High Energy Physics, Ecole des Mines de Nantes, France, 1997 (hep-ph/9706255).